Nuclear Theory – Nuclear astrophysics

J.W. Holt

Introduction

The structure, phases, and dynamics of nuclear matter are crucial to understand stellar explosions, the origin of the elements, patterns in observed gravitational waves, and the composition of the densest observable matter in the universe. The appropriate tool to study strongly interacting matter at the typical scales relevant in nuclear astrophysics (well below the scale of chiral symmetry breaking $\Lambda_\chi \approx 1$ GeV) is chiral effective field theory (ChEFT) [1-3]. In recent years, ChEFT has become a cornerstone of the modern approach to nuclear many-body dynamics that provides a systematic framework for describing realistic microphysics, such as multi-pion exchange processes and three-body forces, within a well-defined organizational hierarchy. The long and intermediate-range parts of the nuclear potential result from one- and two-pion exchange processes, while short-distance dynamics, not resolved at the wavelengths corresponding to typical nuclear Fermi momenta, are introduced as contact interactions between nucleons. Chiral effective field theory is unique in its multichannel methods for quantifying uncertainties and especially in its ability to estimate the importance of missing physics.

Resonant shattering flares as asteroseismic tests of chiral effective field theory

Neutron stars provide a compelling laboratory to test models of the strong interaction in regimes of density and composition (i.e., proton fraction) that are largely inaccessible to terrestrial experiments. In recent years, it has been suggested [4-6] that neutron star normal modes may be probed through gravitational wave observations. In particular, the interfacial *i*-mode is a type of oscillation that occurs at the boundary between different layers of the star, e.g., the crust-core boundary. The *i*-mode is therefore sensitive to properties of neutron stars somewhat below normal nuclear densities and large neutron fraction. It has been hypothesized [7, 8] that if the *i*-mode is excited at its resonant frequency during the late-inspiral stage of binary neutron star coalescence, the crust can shatter and produce a brief flare of gamma rays that takes place before the primary short-hard gamma ray burst that accompanies the merger. Indeed, a number of precursor flares to short gamma-ray bursts have already been observed, e.g., Refs. [9, 10]. If a precursor flare can be observed in coincidence with the gravitational wave signal from a binary neutron star merger, than a precise constraint on the *i*-mode frequency can be obtained by matching to the frequency of the gravitational wave radiation.

In a recent work [11], we have analyzed the possible constraints that a well measured *i*-mode frequency can have on the nuclear equation of state and nuclear force model. We find that measuring the *i*-mode's frequency would provide a meaningful test of ChEFT at densities around half the saturation density. Conversely, we used nuclear matter properties predicted by chiral effective field theory to estimate that the *i*-mode's frequency to be around 185 ± 50 Hz. Asteroseismic observables such as resonant phase shifts in gravitational-wave signals and multi-messenger resonant shattering flare timings, therefore, have the potential to provide useful tests of chiral effective field theory.

In Fig. 1 we show the constraints on the density-dependent nuclear symmetry energy $S_v(n)$ that can be inferred through hypothetical observations of the neutron star *i*-mode with frequency 140 Hz (right panel) and 410 Hz (right panel), both with assumed uncertainties of ± 15 Hz. The broad prior symmetry

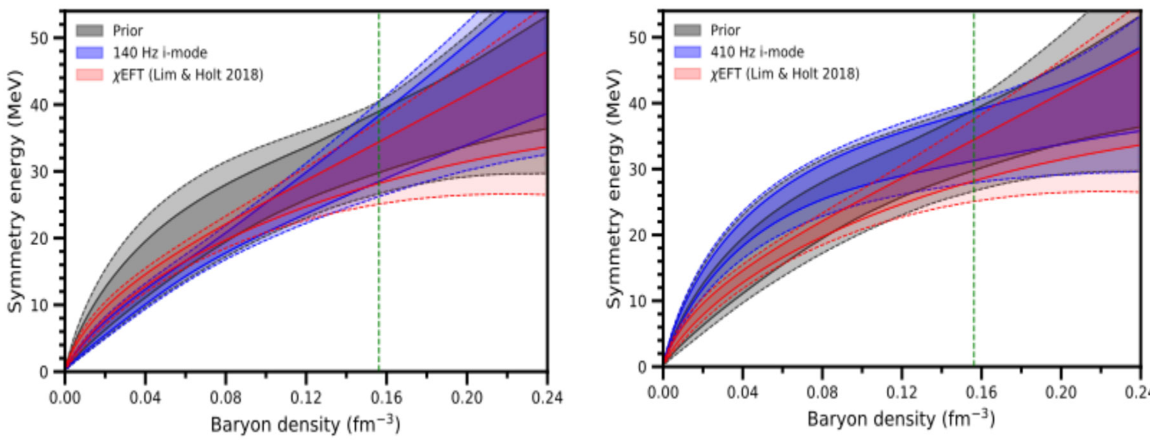

Fig. 1. Prior (grey) and posterior (blue) constraints on the nuclear symmetry energy over the range of densities used by our model, showing what could be learned from measurements of the i-mode frequency. The left panel is for an injected i-mode frequency measurement of 140 Hz, and the right panel for 410 Hz. Also shown (in red) are conservative constraints from chiral effective field theory. Solid (dashed) lines bound the central 68% (95%) credibility regions. The vertical dashed line indicates the nuclear saturation density used in our neutron star model.

energy distribution (gray band) is taken from a meta-model based on Skyrme effective interactions, while the predictions from ChEFT are shown in red. In the left panel, one sees that for a measured *i*-mode frequency of 140 Hz, the symmetry energy posterior distribution is significantly shifted toward lower values in the vicinity of half saturation density $\frac{1}{2}n_0$, which would be consistent with predictions from chiral effective field theory. In addition, such a measurement would rule out a non-trivial fraction of the ChEFT models. On the other hand, the *i*-mode measurement would have a much smaller impact on the symmetry energy at higher densities, where the uncertainties are large. In the right panel of Figure 1, we see that a large measured value of the *i*-mode frequency of 410 Hz would shift the symmetry energy posterior distribution to quite large values around $S_v(n_0/2) = 22 - 30$ MeV. This would rule out a significant fraction of ChEFT models, and therefore we find that a well-measured i-mode frequency has the potential to well constrain the nuclear symmetry energy and models of the nuclear force based on ChEFT.

Correlations between neutron driplines and neutron star properties

One of the central goals of rare-isotope beam facilities is to elucidate the properties of neutron-rich nuclei, which may lead to additional insights into the nuclear equation of state, the nuclear symmetry energy, and neutron star physics. The symmetry energy is closely connected to the limits of nuclear stability, and especially the neutron dripline. Here larger symmetry energies lead to driplines at lower neutron number. At the same time, the symmetry energy is strongly correlated with bulk neutron star properties, such as radii and tidal deformabilities. In a recent work [12], we have investigated the influence of the nuclear symmetry energy and its density slope parameter on the neutron dripline and neutron star properties using a semi-classical liquid drop model (LDM) and energy density functionals constrained by chiral effective field theory. To analyze finite nuclei and mass tables, the nuclear symmetry energy at saturation density is fixed, and the surface tension is determined to minimize the root-mean-square deviation of the total binding energy for 2208 nuclei. Correlations between symmetry energy parameters and neutron driplines, crust-core transition densities, and the radii of $1.4M_{\odot}$ neutron stars are explored using the LDM framework. Additionally, we examined the relationship between macroscopic properties, such as neutron star radii (R1.4), and microscopic properties, including the number of isotopes and the last bound nucleus for Z = 28, within the LDM context.

In Figure 2 we show the correlation between the mass number of the nickel neutron dripline isotope and the radius of a $1.4M_{\odot}$ neutron star for 61 different equations of state. In general, a large symmetry

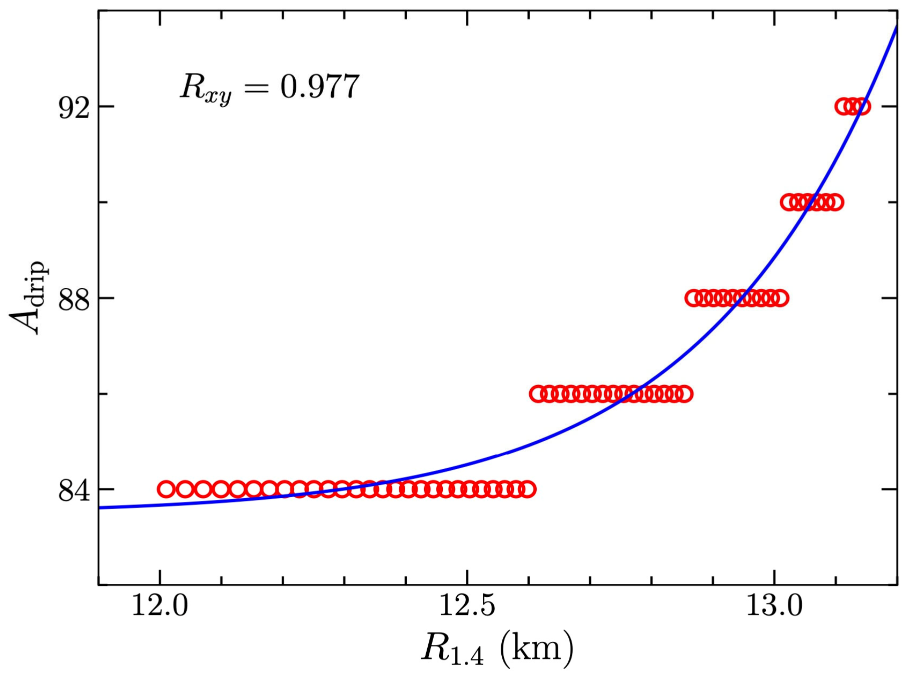

Fig. 2. Correlation between the mass number of the nickel neutron dripline and the radius of a 1.4M_⊙ neutron star.

energy slope parameter is correlated with higher symmetry energies at high density but lower symmetry energies at the small densities characteristic of neutron skins. Therefore, one finds that the neutron star radius, which is positively correlated with the symmetry energy slope parameter, is also positively correlated with larger mass dripline isotopes. We have developed an algebraic model to describe the relationship, which is shown as the blue solid curve and given by the equation

$$A_{\rm drip} = a + b\left(\frac{R_{1.4}}{12\ \rm km}\right)^{\alpha},$$

where $\alpha = 40$. This interesting correlation may be used in the future to place constraints on neutron star radii from laboratory measurements of neutron driplines in medium-mass isotopes.

[1] S. Weinberg, Physica A **96**, 327 (1979).
[2] E. Epelbaum, H.-W. Hammer and U.-G. Meissner, Rev. Mod. Phys. **81**, 1773 (2009).
[3] R. Machleidt and D. R. Entem, Phys. Rep. **503**, 1 (2011).
[4] N. Andersson and W.C.G. Ho, Phys. Rev. D **97**, 023016 (2018).
[5] G. Pratten, P. Schmidt, and T. Hinderer, Nature Comm. **11**, 2553 (2020).
[6] G. Pratten, P. Schmidt, and N. Williams, Phys. Rev. Lett. **129**, 081102 (2022).
[7] D. Tsang, J.S. Read, T. Hinderer, A.L. Piro, and R. Bondarescu, Phys. Rev. Lett. **108**, 011102 (2012).
[8] D. Neill, D. Tsang, H. van Eerten, G. Ryan, and W.G. Newton, MNRAS **514**, 5385 (2022)
[9] A.A. Abdo *et al.*, Nature (London) **462**, 331 (2009).
[10] E. Troja, S. Rosswog, and N. Gehrels, Astrophys. J. **723**, 1711 (2010).
[11] D. Neill, D. Tsang, C. Drischler, J.W. Holt and W. Newton, Phys. Rev. C **111**, 015809 (2025).
[12] Y. Lim and J.W. Holt, arXiv:2502.19762.